Extending femtosecond laser superfilamentation in air with a multifocal phase mask

Silin Fu, André Mysyrowicz, Leonid Arantchouk, Magali Lozano, Aurélien Houard

Extending femtosecond laser superfilamentation in air with a Multifocal Phase Mask

Silin Fu[1,2], André Mysyrowicz[2], Leonid Arantchouk[2], Magali Lozano[2] and Aurélien Houard[2,*]

[1]School of Nuclear Science and Technology, Lanzhou University, Lanzhou 730000, China
[2]Laboratoire d'Optique Appliquée, ENSTA Paris, CNRS, Ecole polytechnique, Institut Polytechnique de Paris, 91162 Palaiseau, France
***Author to whom correspondence should be addressed:** aurelien.houard@ensta.fr

Laser filamentation is a spectacular phenomenon, where self-focusing of the laser pulse generates ionizing light channels. Many applications of filamentation, such as the laser lightning rod, require the generation of superfilaments, long plasma channels of higher electron density than normal filaments. Using a multifocal phase mask, we demonstrate an extension of the superfilamentation length of a focused terawatt laser beam. Optimized superfilaments show an increased energy deposition compared to a normal gaussian beam and an extension of their length by at least a factor two. When put in contact with a high voltage electrode, the guiding of a single plasma column with a length of ~1 m is observed. The length of an air waveguide generated by a vortex laser pulse is also increased by a factor 2 in the presence of the phase mask.

When ultrashort pulses propagate in air, a phenomenon called filamentation occurs if their peak power P exceeds a critical value P_{cr} of a few Gigawatts[1]. In this process, the Kerr effect leads to the self-focusing of the beam until nitrogen and oxygen molecules undergo multiphoton absorption and ionize to form a plasma. Then a defocusing effect caused by the plasma hinders the collapse of the beam. The ensuing dynamic competition between self-focusing, plasma defocusing and other nonlinear effects enables the laser pulse to maintain a very high intensity over a long distance, leaving in its wake a continuous plasma channel[2-4].

By manipulating these light filaments, various applications can be achieved. For instance, terahertz[5,6] or microwaves sources[7,8], backward-propagating air lasing for remote sensing[9,10], drilling holes through cloud for optical communication[11,12], air waveguides for optical[13-15] and plasma waveguides for microwave radiation[16], actuator for supersonic vehicles[17] as well as laser-guided lightning have been reported[18]. These applications rely on two crucial parameters of the filaments: the density and the length of the plasma column.

Regarding the filament plasma density, previous studies have indicated that when $P \gtrsim P_{cr}$, the collimated beam collapses to form a single filament with a clamped laser intensity around $5\text{x}10^{13}$ W/cm^2 and a plasma density around 10^{16} e$^-$.cm^{-3} (for a laser at 800 nm)[19]. When $P \gg P_{cr}$, modulation instabilities lead to the formation of an assembly of random filaments[20]. If the beam is focused, these multiple filaments can merge to self-organize in narrow superfilaments, where the laser intensity increases beyond the clamping intensity, and the electron density exceeds significantly the normal filament density[21-25].

Concerning the length of the plasma strings, when $P \gtrsim P_{cr}$, it is limited to a meter scale by the plasma recombination time[26,27]. When $P \gg P_{cr}$, the multiple plasma strings extend the plasma region to several tens of meters[3]. The length of superfilaments generated plasma is expected to be short, due to the high plasma density further reducing their recombination time. In order to increase the plasma length researchers have split the beam into multiple beams and focused them at different distances[28-30]. Alternatively, a "broken lens" focusing the beams at different positions can create a series of concatenated filaments[31]. However, these methods require complex focusing optics and time-delay control systems. Furthermore, these methods prevent intricate filament structures, such as those produced by vortex laser pulses.

In this letter, we report a simple method to significantly increase the plasma length even in the regime of superfilamentation by adding a multifocal phase mask (MPM) in the path of the laser pulse. A comparison with and without the phase mask reveals a more efficient deposition of the laser energy. This extended superfilament could guide a plasma column over nearly 1 m when it was put in contact with a high voltage electrode. We also show that the phase mask is compatible with a laser pulse having a vortex phase. The length of the air waveguide produced by this vortex filament is then increased by a factor 2.

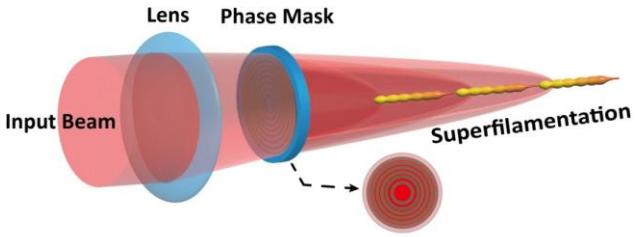

FIG. 1. Setup for generating extended laser superfilamentation.

The principle of the experiment is illustrated in Fig. 1. A focused laser beam is partially diffracted in a phase mask (Holo/Or). This allows the incident beam to be focused at multiple focal distances along the axis of propagation with equivalent laser energy[32]. The laser used is a Ti:Sa CPA laser system from Amplitude. It delivers laser pulses at a repetition rate of 10 Hz with a center wavelength of 800 nm, a minimum pulse duration of 50 fs, and a maximum energy per pulse of 200 mJ. In our experiments, the diameter of the beam was limited to 22 mm (FWHM) by the phase mask aperture. To protect the phase mask, we chose a pulse duration of 500 fs with a positive chirp and a single pulse energy of 120 mJ (92 mJ for the air waveguide experiment). Experiments were conducted with a focusing lens of focal f = 2 m (N.A. = 0.01) for the guided discharges and f = 4 m (N.A. = 0.005) for the air waveguide.

To distinguish the effects of multiple on-axis focusing, we characterized the filaments generated by a pulse of 120 mJ energy ($P \gg P_{cr}$) with and without the phase plate and compared them to a normal single filament produced by a pulse of 10 mJ energy ($P \gtrsim P_{cr},$). Two methods were used to detect the presence of plasma. The first method detected the side fluorescence of the plasma with a CMOS camera placed 40 cm away from the filament. The second used a wide-bandwidth microphone (GRAS Model 46BH 1/4') placed 30 mm away from the filament. This microphone measures the lateral pressure wave generated by fast laser energy deposition, which is roughly proportional to the energy in the plasma[33]. Results are shown in Fig. 2. With an incident pulse of 10 mJ energy, the plasma luminescence signal gives a signal corresponding to the clamped plasma density $n \sim 10^{16}$ $e^{-}.cm^{-3}$ of a normal filament. The width of the plasma column, shown in Fig. 2(a**)** is ~ 100 µm, in agreement with previous reports[1]. Between z = -15 cm and z = 10 cm, the plasma luminescence signal of the 120 mJ pulse is approximately 5 times higher. It corresponds to an increased plasma density, typical of superfilaments[21]. The width of the superfilament plasma column, recorded in a single laser shot and shown in Figure 2(b) is also ~ 100 µm. Note that it is surrounded by a zone of lower plasma density. In the presence of the multifocal phase mask, three peaks are observed in the range from z = -25 cm to z = 20 cm, corresponding to the three focal positions. The magnitude of the luminescence signal over this range indicates the presence of three merged superfilaments.

The deposited energy was measured with and without the phase mask for different incident pulse energies with a focusing lens of 2 m and 3 m. The filaments produced with the phase mask deposited on average about 50% more energy than supergaussian beam with the same input energy. This means that it allows obtaining a more uniform energy distribution along the laser axis and also increases the percentage of ionizing laser energy. This explains why the peak signal of the extended superfilamentation does not decrease significantly when compared to a typical superfilament.

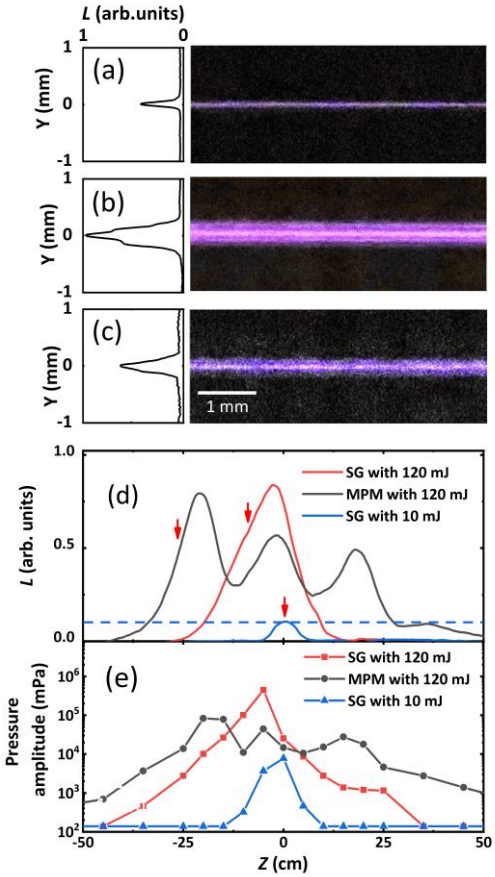

FIG. 2. Comparison between a regular filament, a typical superfilament, and an extended superfilament. (a), (b), (c) and (d) are plasma luminescence signals measured by a commercial camera in a single laser shot. (a) supergaussian (SG) pulse with 10 mJ energy, (b) same pulse with 120 mJ, (c) same pulse with 120 mJ but with the phase mask. (d) axial plasma luminescence integrated L over ten laser shots. The red arrows in (d) correspond to the positions of the measurements in (a), (b) and (c). (e) amplitude of the radial acoustic wave measured by a microphone positioned 30 mm away from the laser axis for the same cases as in subfigure (d) as a function of position z along the laser propagation axis. Position z = 0 corresponds to the geometrical focus of the beam of numerical aperture N.A. = 0.01. The dotted horizontal line in (d) gives the magnitude of a clamped plasma.

We tested the potential of this extended superfilamentation for the guiding of electrically charged plasma columns[34]. Using a pulsed Tesla generator providing a 315 kV voltage pulses on a sharp electrode, we observed the length of the plasma when it was put in contact with the tip of the charged electrode. The pointed Tesla electrode was placed at the geometrical focus of the beam. Without laser or with a single filament (10 mJ), only the radiation from small erratic streamer discharges of a few centimeters was observed around the electrode. The plasma luminescence of a superfilament in absence of high voltage and MPM, integrated over 10 shots, is shown in Fig. 3(a), 3(b). In the presence of high voltage, a charged plasma column of approximately 40 cm was observed, which is twice the length of the superfilament. (Fig. 3(a), (c)). In the presence of the phase mask and of the high voltage, the extended laser superfilaments shown in Fig. 3(d), (e), allows the guiding of a single continuous plasma column of 86 cm length (Fig. 3(d), (f)). As discussed in ref. 35, this guiding occurs because the plasmas expand very rapidly along the long-lived low-pressure track left in the wake of the propagating filamentary pulse[36].

An interesting application of filamentation is the production of remote optical waveguides. Similar to a step index fiber, an air waveguide can be used for the transport of nanosecond laser pulses, or for the remote collection of spectroscopic signals[13]. Remote optical waveguides can be formed when multiple filaments produced by a laser pulse generate pressure waves converging to the laser beam axis to form a high-pressure zone hundreds of microseconds after the passage of the laser pulse. Optical air waveguides are obtained by dividing the beam profile into several discontinuous phase sectors or by generating a beam with a vortex phase. We used our phase mask to increase the

length of air waveguides generated by vortex filaments. The filamentation of a vortex beam can create multiple parallel filaments. After few hundreds microseconds, heating of the gas in the filaments evolves into a higher gas density on axis[14,15]. We found that it is very difficult to generate multiple superfilaments with vortex beams because of risk of damage of the vortex phase plate. Therefore, this section is discussed only in the context of regular filaments. To generate the vortex beam we used a vortex phase plate with a topological charge m = 8. The laser energy was fixed at 92 mJ and the beam was weakly focused in air through a lens with a focal length of f = 4000 mm (N.A. = 0.005). We first measured the acoustic signals generated by both normal vortex filaments and extended vortex filaments, as shown in Fig. 4. For the vortex filaments an acoustic signal is observed between z = -150 cm and z = 200 cm. In contrast, with the extended vortex filaments the plasma goes from z = -225 cm to z = 450 cm, indicating that the phase mask also doubled the length of the vortex filaments, suggesting that it can also extend the length of air waveguides.

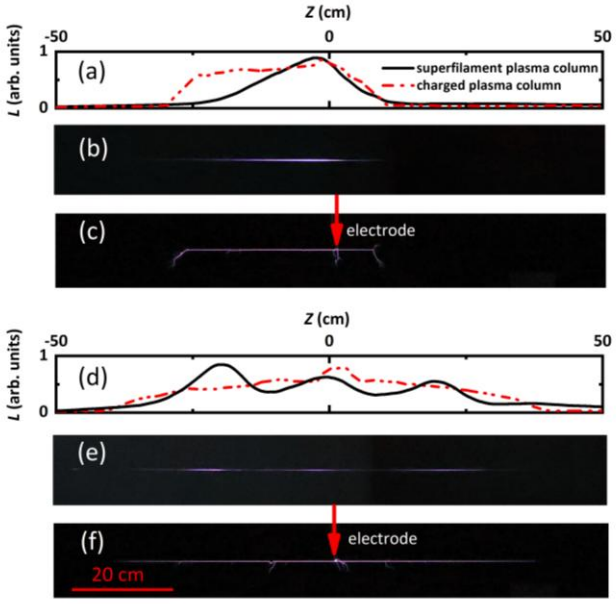

FIG. 3. Comparison of plasma length obtained with and without applied voltage using a typical superfilament and extended superfilamentation. (a) On axis luminescence signal of the laser superfilament (black curve) and of the charged plasma channel (red dashed curve) as a function of the propagation distance. (b) Plasma luminescence of a typical superfilament without applied voltage recorded over 10 laser shots. (c) Plasma luminescence of a typical charged plasma channel with applied voltage recorded in a single laser shot. (d) Same as a but with phase mask. (e). Same as (b) but with phase mask. (f). same as c but with phase mask. The estimated width of the plasma channel is < 100 μm. The laser energy is 120 mJ, and the focusing lens is f = 2000 mm. The pointed electrode is placed at z = 0. The laser is propagating from left to right and the camera is at a distance of 1 m from the plasma.

We conducted air waveguide tests using as a probe beam a Yb:YAG laser pulse at 532-nm with an energy in the μJ-level and a pulse duration of 10 nanoseconds. The delay between the femtosecond and nanosecond laser pulse could be controlled using a delay generator. A dichroic mirror was used to combine the two beams. The profile of the 532-nanometer probing beam was captured by a CMOS camera located 10 meters behind the lens, with a color filter to block the light from the fs laser at 800-nm (See description of the setup in detail in ref 14). In previous studies, we determined that the efficiency of this air waveguide is highest at a delay of 500 μs after the formation of the filament. In the Fig. 4 (c-d), we present the profile of the probing pulse sent 500 μs after the generation of the filament, as captured by the CMOS camera for three different cases: b) in the absence of filaments, c) in the presence of filaments generated by the vortex phase-plate and d) in the presence of filaments generated by the vortex phase and the multifocal phase mask. One can see that the diameter of the guided beam measured 6 meters after the lens geometrical focus is almost 2 cm without air waveguide, is 6.4 mm at the output of the air waveguide alone and is almost two times smaller in the case of the extended vortex beam (3.2 mm width). This corresponds to the diffraction of a guided beam with a diameter of 0.8 mm FWHM going out of the waveguide at z = 150 cm without MPM and at z = 350 cm with the MPM. The air waveguide is therefore extended by 2 m in the presence of the MPM.

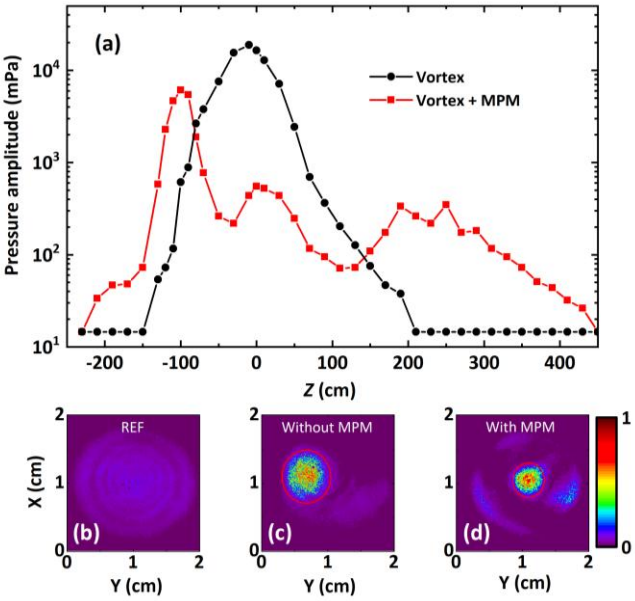

FIG. 4. Air waveguide produced by the filaments. (a) Amplitude of the transverse acoustic wave measured by a microphone 30 mm away from the laser filament axis. The laser beam has an energy of 92 mJ, a duration of 500 fs and a vortex topological charge m = 8. (b-d) profile of the probe beam measured at z = 10 m at the output of the air waveguide, in the absence of filament (b), in the presence of filaments generated by the vortex phase-plate (c), and in the presence of filaments generated by the vortex phase and the MPM (d). The probe beam is sent 500 μs after the fs laser pulse.

In this study, the length of laser superfilaments was extended by a factor two using a multifocal phase mask. Through measurements of acoustic signals and deposited energy, we demonstrated that this method leads to a more efficient deposition of energy along the laser path, when compared to normal focusing modes, while maintaining a high laser intensity. We also demonstrated that the multifocal mask can expand the guided length of a charged plasma column to almost 1 m. By combining this method with a vortex beam, the length of the generated air waveguide was also doubled. We believe this phase mask method has the potential to be useful in atmospheric applications sensitive to filament plasma lengths, such as lightning control[18], optical communication through fog and cloud layers[11], satellite communication[37] and filament waveguiding[15,16] over longer distances.

ACKNOWLEDGMENTS

We acknowledge technical support from Y.-B. André and from the workshop of LOA for the development of the high voltage generator.

DATA AVAILABILITY

Data underlying the results presented in this paper are not publicly available at this time but may be obtained from the authors upon reasonable request.

REFERENCES

1. A. Couairon, and A. Mysyrowicz, "Femtosecond filamentation in transparent media," Phys. Rep. **441**, 47-189 (2007).
2. M. Rodriguez, R. Bourayou, G. Méjean, *et al.* "Kilometer-range nonlinear propagation of femtosecond laser pulses," Phys. Rev. E **69**, 036607 (2004).
3. M. Durand, A. Houard, B. Prade *et al.* "Kilometer range filamentation," Optics Express **21**, 26836 (2013).
4. P. Walch, B. Mahieu, V. Moreno *et al.* "Long distance laser filamentation using Yb:YAG kHz laser," Sci. Rep. **13**, 18542 (2023).

5. C. D'Amico, A. Houard, M. Franco et al. "Conical forward THz emission from femtosecond laser filamentation in air," Phys. Rev. Lett. **98**, 235002 (2007).
6. A. D. Koulouklidis, C. Gollner, V. Shumakova *et al.* "Observation of extremely efficient terahertz generation from mid-infrared two-color laser filaments," Nat Commun **11**, 292 (2020). https://doi.org/10.1038/s41467-019-14206-x
7. A. Englesbe, J. Elle, R. Schwartz, *et al.* "Ultrabroadband microwave radiation from near- and mid-infrared laser-produced plasmas in air," Phys. Rev. A **104**, 013107 (2021).
8. A. M. Zheltikov, "Laser filaments as pulsed antennas," Opt. Lett. **46**, 4984-4987 (2021).
9. A. Dogariu, J. B. Michael, M. O. Scully, and R. B. Miles, "High-gain backward lasing in air," Science **331**, 442–445 (2011).
10. H. Xu, E. Lötstedt, A. Iwasaki, K. Yamanouchi, "Sub-10-fs population inversion in N_2^+ in air lasing through multiple state coupling," Nat. Commun. **6**, 8347 (2015).
11. G. Schimmel, T. Produit, D. Mongin, J. Kasparian, & J.-P. Wolf, "Free space laser telecommunication through fog," Optica **5**, 1338-1341 (2018).
12. S. B. Ali Reza, M., Burger, P. Bassène, T. Nutting, I. Jovanovic, and M. N'Gom, "Generation of multiple obstruction-free channels for free space optical communication," Opt. Express **31**, 3168-3178 (2023).
13. N. Jhajj, E. W. Rosenthal, R. Birnbaum, J. K. Wahlstrand, and H. M. Milchberg, "Demonstration of long-lived high-power optical waveguides in air," Physical Review X **4**, 011027 (2014).
14. S. Fu, B. Mahieu, A. Mysyrowicz and A. Houard, "Femtosecond filamentation of optical vortices for the generation of optical air waveguides," Opt. Lett. **47**, 5228-5231 (2022).
15. A. Goffin, I. Larkin, A. Tartaro, *et al.* "Optical Guiding in 50-Meter-Scale Air Waveguides," Phys. Rev. X **13**, 011006 (2023).
16. M. Châteauneuf, S. Payeur, J. Dubois, and J.-C. Kieffer, "Microwave guiding in air by a cylindrical filament array waveguide," Appl. Phys. Lett. **92**, 091104 (2008).
17. P.-Q. Elias, N. Severac, J.-M. Luyssen, *et al.* "Improving supersonic flights with femtosecond laser filamentation," Science Advances **4**, eaau5239 (2018).
18. A. Houard, P. Walch, T. Produit, *et al*. "Laser-guided lightning," Nat. Photonics **17**, 231 (2023).
19. A. Becker, N. Aközbek, K. Vijayalakshmi, *et al.* "Intensity clamping and re-focusing of intense femtosecond laser pulses in nitrogen molecular gas," Appl. Phys. B **73**, 287–290 (2001).
20. M. Mlejnek, M. Kolesik, J. V. Moloney, & E. M. Wright, "Optically Turbulent Femtosecond Light Guide in Air," Phys. Rev. Lett. **83**, 2938 (1999).
21. G. Point, Y. Brelet, A. Houard *et al.* "Superfilamentation in Air," Phys. Rev. Lett. **112**, 223902 (2014).
22. K. Lim, M. Durand, M. Baudelet & M. Richardson, "Transition from linear- to nonlinear-focusing regime in filamentation," Sci. Rep. **4**, 7217 (2014).
23. Z. Samsonova, D. Kartashov, C. Spielmann, *et al.* "Measurements of fluence profiles in femtosecond laser sparks and superfilaments in air," Phys. Rev. A **97**, 063841 (2018).
24. A. Murzanev, S. Bodrov, Z. Samsonova, D. Kartashov, M., Bakunov, & M. Petrarca, "Superfilamentation in air reconstructed by transversal interferometry," Phys. Rev. A **100**, 063824 (2019).
25. D. Pushkarev, E. Mitina, D. Shipilo *et al.* "Transverse structure and energy deposition by a subTW femtosecond laser in air: from single filament to superfilament," New J. Phys. **21** 033027 (2019).
26. S. Tzortzakis, B. Prade, M. Franco, A. Mysyrowicz, "Time-evolution of the plasma channel at the trail of a self-guided IR femtosecond laser pulse in air," Opt. Commun. **181**, 123 (2000).
27. Y. Chen, F. Théberge, O. Kosareva, N. Panov, V. P. Kandidov, and S. L. Chin, "Evolution and termination of a femtosecond laser filament in air," Opt. Lett. **32**, 3477-3479 (2007).
28. S. Tzortzakis, G. Méchain, G. Patalano, *et al.* "Concatenation of plasma filaments created in air by femtosecond infrared laser pulses," Appl. Phys. B **76**, 609–612 (2003).
29. P. Polynkin, "Multi-pulse scheme for laser-guided electrical breakdown of air," Appl. Phys. Lett. **111**, 161102 (2017).
30. P. Polynkin, Z. Samsonova, A. Englesbe, A. Lucero, J. Elle, & A. Schmitt-Sody, "Channeling the dielectric breakdown of air by a sequence of laser-generated plasma filaments," JOSA B **36**, 3024 (2019).
31. J. Papeer, R. Bruch, E. Dekel, *et al.* "Generation of concatenated long high density plasma channels in air by a single femtosecond laser pulse," Appl. Phys. Lett. **107**, 124102 (2015).
32. L. L. Doskolovich, E. A. Bezus, A. A. Morozov, V. Osipov, J. S. Wolffsohn, & B. Chichkov, "Multifocal diffractive lens generating several fixed foci at different design wavelengths," Opt. Express **26**, 4698-4709 (2018).
33. J. Yu, D. Mondelain, J. Kasparian *et al.* "Sonographic probing of laser filaments in air," Appl. Opt. **42**, 7117-7120 (2003).
34. T.J. Wang, Y. Wei, Y. Liu *et al.* "Direct observation of laser guided corona discharges," Sci. Rep. **5**, 18681 (2016).
35. L. Arantchouk, M. Lozano, Y.-B. André *et al.* "Evolution of a charged plasma column created by femtosecond superfilamentation," In preparation (2023).
36. Footnote: Note the presence of small lateral streamers in charged plasma and a small deviation from rectilinear path around z = -10 cm, at the junction between the first and second superfilaments.
37. I. Dicaire, V. Jukna, C. Praz, C. Milián, L. Summerer, and A. Couairon, "Spaceborne laser filamentation for atmospheric remote sensing," Laser & Photonics Reviews **10**, 481-493 (2016).